Aromatization of methane in the absence of oxygen over Mo-based catalysts supported on different types of zeolites

Chun-Lei Zhang [a,b], Shuang Li [a,*], Yi Yuan [a], Wen-Xiang Zhang [a], Tong-Hao Wu [a] and Li-Wu Lin [b]

[a] *Department of Chemistry, Jilin University, Changchun 130023, PR China*
[b] *State Key Laboratory for Catalysis, Dalian Institute of Chemical Physics, Chinese Academy of Sciences, PO Box 110, Dalian 116023, PR China*

Received 11 August 1998; accepted 10 November 1998

The catalytic performance of Mo-based catalysts supported on various zeolites has been studied for methane aromatization in the absence of oxygen in a fixed-bed continuous-flow quartz reactor, and their catalytic properties are correlated with features of zeolite structure. It was found that H-type silica–alumina zeolites, such as ZSM-5, ZSM-8, ZSM-11 and β possessing two-dimensional structure and pore diameter equaling the dynamic diameter of a benzene molecule (about 6 Å) simultaneously, are fine supports for methane activation and aromatization catalysts. Among them, MoO_3/H-ZSM-11 has the best activity and stability; for instance, a methane conversion of 8.0% and selectivity higher than 90% was obtained at 973 K. The catalytic performance of MoO_3/H-ZSM-8 is somewhat lower than that of MoO_3/H-ZSM-5, while activity of MoO_3/H-β is lower than that of MoO_3/H-ZSM-8. Catalysts supported on H-MCM-41 and H-SAPO-34 exhibit low activity for methane aromatization and those supported on H-MOR, H-X and H-Y give only a little amount of ethylene. Over MoO_3/H-SAPO-5 and MoO_3/H-SAPO-11 no hydrocarbons were detected.

Keywords: zeolite structure, methane aromatization, MoO_3, benzene, shape-selective function

1. Introduction

Methane dehydrogenation in the absence of oxygen to produce valuable liquid product – aromatics, which is considered as one of the newest results obtained in the studies of methane coupling, is of great theoretical and economic significance [1]. In recent years, most studies have focused on the catalytic performance of Mo-based catalysts supported on H-ZSM-5. Wang and Chen et al. [2–7] reported a 6–8% conversion of methane with selectivity to benzene higher than 80% over MoO_3/H-ZSM-5 catalysts at 973 K. Solymosi et al. [8] found that K_2MoO_4/H-ZSM-5 is also active for methane aromatization reaction and a 1.2–6.3% conversion of methane with 60% selectivity to benzene was achieved. Recently, Lunsford [9] and Solymosi et al. [10] reported a 5–7% methane conversion with selectivity higher than 70% over Mo_2C/H-ZSM-5 and considered that carbidic molybdenum species were the active centers for the activation of methane. In addition, studies on catalyst promoters, such as Pt, Ru, WO_3, etc. [11–13] were also reported. However, as far as catalyst support is concerned, only H-ZSM-5, SiO_2, Al_2O_3 and SAPO-34 were used, and the last two have relatively low activity and selectivity [13–15]. Up to now, studies on using other types of zeolites as supports have not been reported. In the present paper, the catalytic performance of Mo-based catalysts supported on zeolites with different structures was studied, and the relationship between the catalytic behavior and the structural characteristics of these zeolites was discussed. Some distinguished structural features of fine supports for this reaction were found and optimization for catalysts was also carried out.

* To whom correspondence should be addressed.

2. Experimental

2.1. Synthesis of zeolites and preparation of catalysts

2.1.1. Pretreatment of H-ZSM-5

H-ZSM-5 (supplied by Nankai University with SiO_2/Al_2O_3 = 25 and 50) was pretreated as follows: first calcined at 773 K for 4 h in air, then boiled in water for 4 h, followed by ion exchange with a 1 N NH_4NO_3 aqueous solution at about 368 K, the obtained zeolite precursor was dried at 393 K and calcined at 773 K for 4 h.

2.1.2. Synthesis of H-ZSM-8

H-ZSM-8 (SiO_2/Al_2O_3 = 50) was synthesized by the procedure given in [16] using TEA^+ as a template. Gels with the following molar composition: $16.5Na_2O{\cdot}6TEA^+{\cdot}1Al_2O_3{\cdot}50SiO_2{\cdot}2150H_2O$ were prepared using NaOH, TEAOH, $Al_2(SO_4)_3$ and SiO_2. For synthesizing the sample the gel was introduced in a teflon-lined stainless-steel autoclave and heated at 433 K for 4 days. The product was filtered, washed and dried to obtain Na-ZSM-8 powder. H-ZSM-8 support was obtained by calcining Na-ZSM-8 at 823 K in air for 8 h to remove the template, and boiling in water for 4 h, followed by four times ion exchange with a 1 N NH_4NO_3 aqueous solution at about 368 K, then drying and calcining at 773 K for 3 h.

2.1.3. Synthesis of H-ZSM-11

H-ZSM-11 ($SiO_2/Al_2O_3 = 25$, 50) was synthesized by the method in [17]. Molar composition of the gel is $9Na_2O{\cdot}1TBA^+{\cdot}1\text{–}2Al_2O_3{\cdot}50SiO_2{\cdot}5000H_2O$. Similar hydrothermal conditions and treatment procedure as for H-ZSM-8 were used.

2.1.4. Synthesis of H-β

Following the procedure reported in [18], we synthesized H-β ($SiO_2/Al_2O_3 = 50$) in the presence of TEA^+ as a template. Using the same feeding order and treatment procedure and by crystallization at 413 K for 120 h, H-β was obtained.

2.1.5. Synthesis of H-MCM-41

H-MCM-41 ($SiO_2/Al_2O_3 = 50$) was synthesized by the method given in [20]. The gels were introduced into a beaker in the order: H_2O, NaOH, $C_{16}H_{33}(CH_3)_3NBr$, SiO_2 and AlO(OH), and stirred 2 h to obtain Na-MCM-41 powder. The product was treated by a same procedure as that for obtaining H-ZSM-8.

2.1.6. Preparation of other types H-form zeolites

H-MOR, H-X and H-Y types of zeolites were supplied by NO.3 Oil Factory, Fushun; and H-SAPO-5, H-SAPO-11 and H-SAPO-34 were supplied by Dalian Institute of Chemical Physics. These zeolites were treated by a same procedure as that for H-ZSM-5.

2.1.7. Preparation of Mo-based catalysts supported on H-form zeolites

A mixture of MoO_3 and zeolite was made by grinding. A prescribed amount of MoO_3 with the above-mentioned synthesized H-form zeolites was thoroughly ground, then calcined at 773 K for 4 h in air.

2.2. Characterization of zeolite structures

XRD patterns were taken with a Shimadzu XD-3A diffractometer using CuK_α radiation, operating at 30 kV, 20 mA, and with a scanning speed of 4°/min at room temperature.

Infrared spectra were recorded at room temperature on a Nicolet Compact 410 spectrometer. Self-supporting wafers were pressed using a mixture of zeolite and KBr.

2.3. Catalytic test

Methane non-oxidative aromatization reactions were carried out in a fixed-bed continuous-flow 8 mm i.d. quartz microreactor. The catalyst charge was 1.0 g (40–60 mesh). It was first heated to reaction temperature in air stream (20 ml/min) at a speed of 20 K/min and then maintained at the reaction temperature in air and helium for 10 min. After pretreatment, pure methane was introduced into the reactor at a space velocity of 1600 ml/g h. The reaction temperature is 973 K. The reaction mixture was analyzed by an online Shimadzu GC-8A gas chromatograph in temperature-programmed mode using a 2 m Porapak Q column and detected with a TC detector. The methane conversion and product selectivity were calculated on a carbon number base without accounting for coking.

3. Results and discussion

3.1. Structure analysis of various zeolites

Figure 1 shows XRD patterns of H-form zeolites with different structures. Obviously, all samples are pure zeolites with corresponding structure without contamination of the secondary phase and have nice crystalline structure. It can also be found that ZSM-5, ZSM-8 and ZSM-11 show similar XRD patterns, the only difference between ZSM-5 and ZSM-8 being that the XRD pattern of ZSM-8 shows a splitting in the highest peak ($d = 3.85$) which is not observed for ZSM-5. The XRD pattern of ZSM-11 does not show splitting at peaks with d value of 3.71 and does not exhibit peaks with d value of about 3.65 as compared with that of ZSM-5.

IR adsorption bands (400–1400 cm^{-1}) of the framework vibration of various zeolites have been investigated (figure 2); the corresponding absorption bands and their assignments, which are based on earlier studies on zeolites in general, are summarized in table 1. It can be seen that all zeolites exhibit very strong absorption within 1000–1100 cm^{-1} and a strong absorption at 450 cm^{-1}. However, the number of IR absorption bands and its wavenumbers vary greatly with the difference in structure of zeolites. By comparison of IR spectra of ZSM-5, ZSM-8 and ZSM-11, it can be found that there is little difference among them, that is, the number of IR absorption bands and their wavenumbers are almost the same, indicating that they have similar framework structure consisting of 5-membered rings. In addition, the link patterns of 5-membered rings are analogous. The absorption bands of X and Y type zeolites in the range of 550–580 cm^{-1} are assigned to double 6-membered rings, while the bands of ZSM-5, ZSM-8 and ZSM-11 at 550 cm^{-1} are ascribed to double 5-membered rings.

3.2. The catalytic performance of methane aromatization reaction over different types of silica–alumina zeolite-supported catalysts

The conversion of methane over Mo-based catalysts supported on H-form zeolites with various structures is given in table 2. Obviously, MoO_3/H-ZSM-11 has the highest activity of all these catalysts at the same Si/Al ratio; its methane conversion reaches 8.0% with a selectivity to benzene higher than 90% at 973 K. The activity of MoO_3/H-ZSM-8 is lower than that of MoO_3/H-ZSM-5 at 973 K. Over MoO_3/H-ZSM-8 a methane conversion of 4.11% is achieved with benzene selectivity of 86.7%. In addition, MoO_3/H-β also shows certain activity for

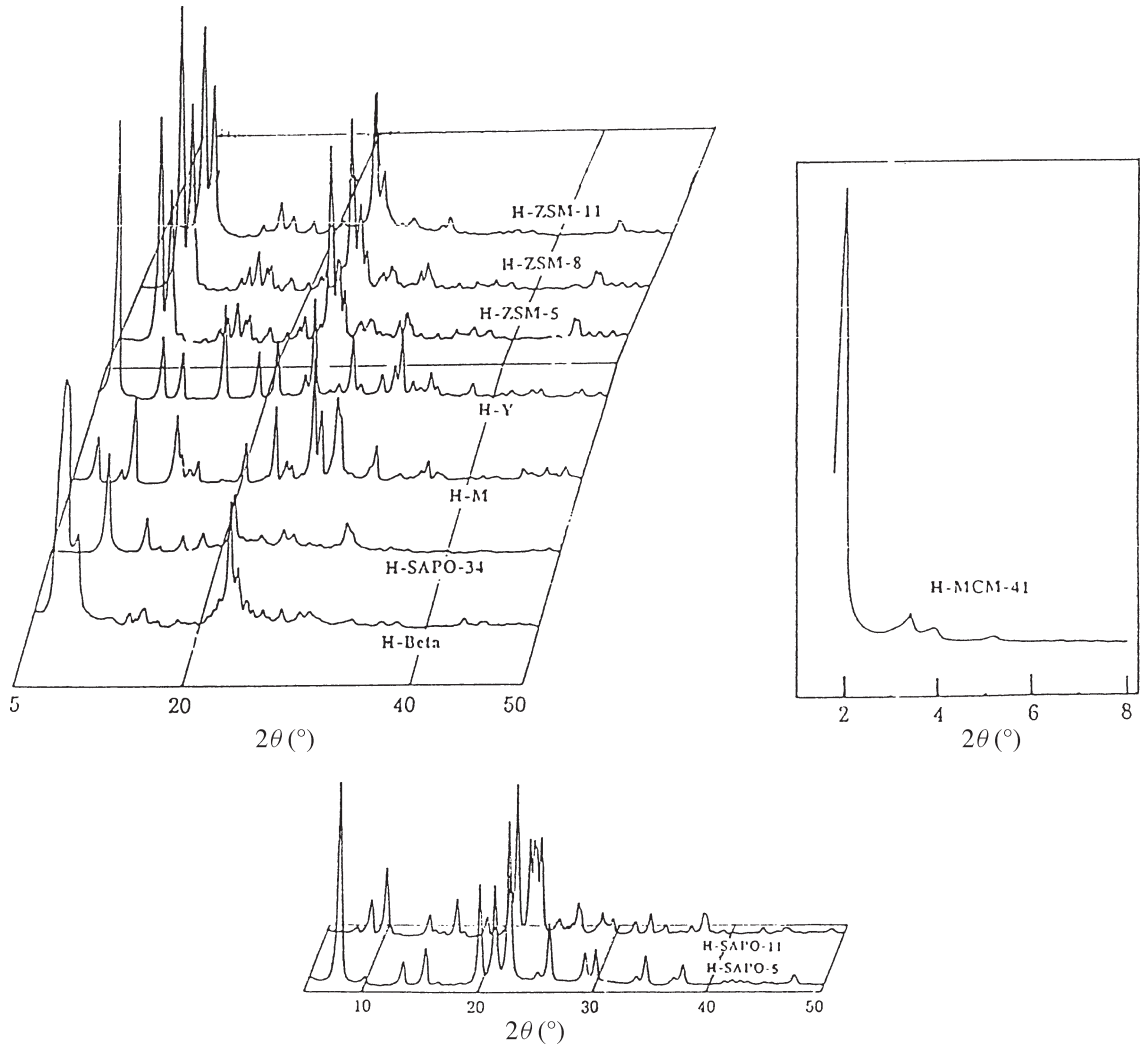

Figure 1. XRD patterns of various H-form zeolites.

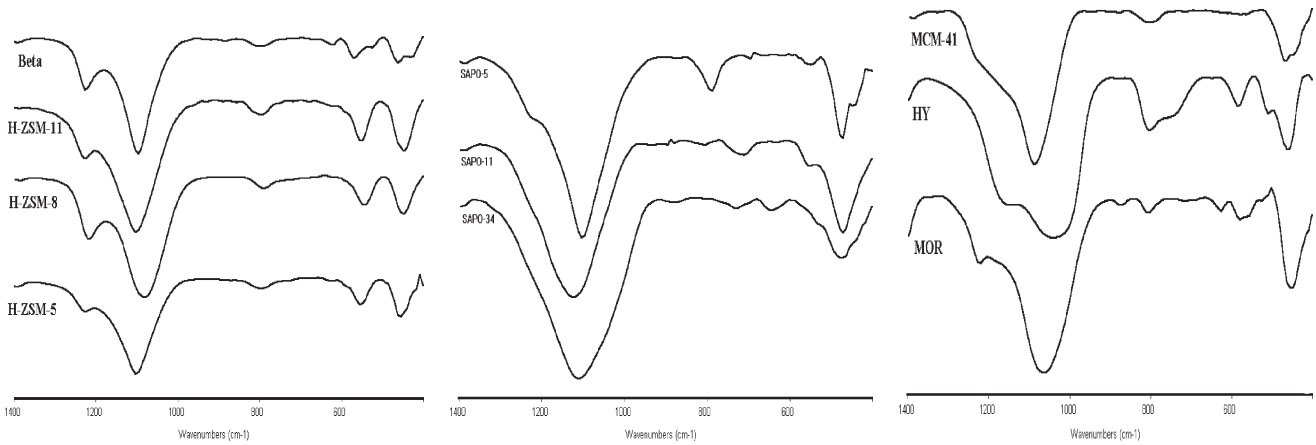

Figure 2. IR spectra of various zeolites.

this reaction. MoO_3/H-MCM-41 and MoO_3/H-SAPO-34 exhibit low activity; benzene selectivities of 80.1 and 70.8% with methane conversion of 0.9 and 0.7% are achieved, respectively. Over MoO_3/H-X and MoO_3/H-Y only a small amount of ethylene is observed and no aromatics is detected. No hydrocarbons are observed over MoO_3/H-SAPO-5 and MoO_3/H-SAPO-11. As can be seen from the above-mentioned results, the activities of catalysts for the reaction are in the following order: MoO_3/H-ZSM-11 > MoO_3/H-ZSM-5 > MoO_3/H-ZSM-8 >

Table 1
Framework vibration absorption bands[a] of zeolites with various structures.

Type of zeolite	TO_4 asymmetric stretching vibration	TO_4 symmetric stretching vibration	Double-ring vibration	T–O band bending vibration
ZSM-5	1222, 1106	797	550	450
ZSM-8	1225, 1101	796	552	447
ZSM-11	1216, 1081	789	544	449
β	1224, 1096, 952	798, 720, 620	569, 527	461, 430
MOR	1221, 1063, 880	801, 625	579	454
MCM-41	1225, 1086	804	563	467, 446
X	1060, 965	745, 685, 665	555	445
Y	1147, 1040	801, 730, 645	583	507, 460
SAPO-5	1225, 1102	789, 685	546	474, 449
SAPO-11	1124, 880	713	553	472
SAPO-34	1118, 872	729, 645	535	476

[a] In cm^{-1}.

Table 2
The activity of 3% MoO_3/zeolite catalysts (reaction temperature 973 K, methane space velocity 1600 ml/g h, $SiO_2/Al_2O_3 = 50$).

Zeolite support	Methane conversion[a] (%)	Selectivity[a] (%)		
		Benzene	C_2	CO
H-ZSM-5	5.9	91.3	4.5	4.2
H-ZSM-5[b]	6.9	90.8	4.3	4.9
H-ZSM-8[c]	4.11	86.7	3.9	9.4
H-ZSM-11[b]	8.0	90.9	5.5	3.6
H-ZSM-11	7.61	91.6	5.3	3.1
H-β[d]	3.11	80.4	8.8	10.8
H-MCM-41	0.9	80.1	8.7	11.2
H-SAPO-34[e]	0.6	72.9	10.1	17
H-MOR	0.8	0	72.3	27.7
H-X	0.7	0	70.1	29.9
H-Y	0.7	0	80.2	19.8
H-SAPO-5	–	–	–	–
H-SAPO-11	–	–	–	–

[a] Without counting for coking.
[b] $SiO_2/Al_2O_3 = 25$.
[c] MoO_3 loading: 6 wt%.
[d] MoO_3 loading: 7 wt%.
[e] Reaction temperature is 923 K.

MoO_3/H-β > MoO_3/H-MCM-41 > MoO_3/H-SAPO-34 > MoO_3/H-MOR ≈ MoO_3/H-X ≈ MoO_3/H-Y > MoO_3/H-SAPO-5 ≈ MoO_3/H-SAPO-11.

The methane conversion with time on stream over various Mo-based H-form zeolite catalysts is shown in figure 3. It can be seen that MoO_3/H-ZSM-11 has relatively higher activity in the whole period of reaction compared with the MoO_3/H-ZSM-5 catalyst and the selectivity to benzene is about the same as that over MoO_3/H-ZSM-5. With reaction time increasing, the reactivity of MoO_3/H-ZSM-8 decreases rapidly, and within 40 min of reaction, large amount of CO is produced. As for the MoO_3/H-β catalyst, with increasing time on stream the methane conversion and selectivity to benzene do not vary greatly. MoO_3/H-SAPO-34 has poor stability, the methane conversion and selectivity to benzene decrease rapidly with increasing time on stream and after 3 h the catalyst exhibits nearly no activity. It is interesting that over 3% MoO_3/H-MCM-41 a very long induction stage of about 4.5 h is needed. As can be seen in figure 3, the H-ZSM-11-, H-ZSM-5- and H-β-supported Mo-based catalysts show relatively high and stable selectivity to benzene during the whole reaction process.

3.3. Correlation of the catalytic performance of catalysts with structure of silica–alumina zeolites

The catalytic performance of Mo-based catalysts supported on zeolites with different structure has been studied. It is found that zeolite structure has great effect on the catalytic performance of the catalysts. In order to clarify the relationship between reaction activity and zeolite structure, we studied the structural features of various zeolites.

The space structures and pore systems of various zeolites are given in table 3. ZSM-5 possesses two-dimensional pore structure, which belongs to orthogonal or monoclinic crystal system. The pore opening is a 10-membered ring. Its pore system consists of an elliptical straight channel with pore diameter of 5.4 × 5.6 Å and sine curve shape channel of 5.1 × 5.5 Å, which intersect each other perpendicularly. ZSM-8 pertains to orthogonal crystal system; the ring of the pore opening is 10-membered. The elliptical straight channel and curved channel intersecting each other perpendicularly form its channel system. ZSM-8 also has two-dimensional structure with average pore diameter about 5 Å. ZSM-11, by contrast, belongs to the tetragonal crystal system; it comprises two straight-line channels that intersect each other perpendicularly with pore aperture of 5.1 × 5.5 Å formed by 10-membered rings. ZSM-11 possesses two-dimensional pore structure just as ZSM-5 and ZSM-8. There exist three crystal systems in β zeolite: tetragonal, anorthic and monoclinic and its crystal structure is highly disordered and has many defects. The pore structure of β zeolite is two-dimensional, which is constituted with an elliptical straight channel with diameter of 6.6 × 8.1 Å and an elliptical curved channel with diameter of 5.5 × 6.5 Å formed by 12-membered rings. Obviously, ZSM-5, ZSM-8 and β zeolite, which show relatively fine activity for methane aromatization under non-oxidative condition, all possess a pore diameter near to the dynamic diameter of a benzene molecule,

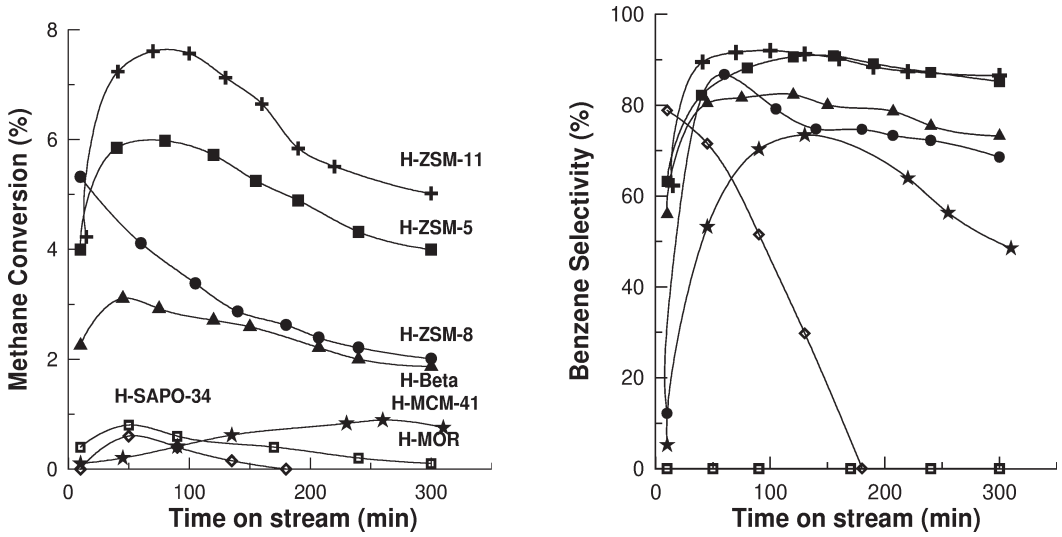

Figure 3. The methane conversion and benzene selectivity over various Mo-based zeolite ($SiO_2/Al_2O_3 = 50$) catalysts at 973 K (except H-SAPO-34) with methane space velocity of 1600 ml/g h.

Table 3
Pore structure and channel systems of zeolites.

Zeolite	Pore diameter (Å)	Ring number of pore opening	Crystal system	Dimensions of pore structure	Pore system
ZSM-5	5.4 × 5.6 5.1 × 5.5	10	orthogonal or monoclinic	II	straight line and Z shape channel
ZSM-8	5^+	10	orthogonal	II	straight line channel
ZSM-11	5.1 × 5.5	10	tetragonal	II	straight line channel
SAPO-5	8	12	hexagonal	III	straight line channel
SAPO-11	6	10	orthogonal	III	straight line channel
SAPO-34	4.3	8	trigonal	III	straight line channel with cage
X	7.4	12	cubic	III	straight line channel with supercage
Y	7.4	12	cubic	III	straight line channel with supercage
MOR	6.6 2.8	12 8	orthogonal	II	straight line channel
β	5.5 × 6.5 6.6 × 8.1	12	tetragonal, anorthic or monoclinic	II	straight line and curved channel
MCM-41	40			I	straight line channel

and all have two-dimensional pore structure. Nevertheless, catalysts showing low or no activity for methane conversion all do not possess or do not possess simultaneously these two structure features: ~6 Å pore diameter and two-dimensional pore structure. For instance, SAPO-34 is a small-pore zeolite with pore diameter of about 4.3 Å and its channel system is a straight channel with cage. Although the pore diameter of SAPO-11 is about 6 Å, it has three-dimensional structure, with relatively large pore diameter of 8 Å. Likewise, octahedral zeolites X and Y are also large-pore zeolites, whose pore system is a three-dimensional straight channel with supercage.

As is well known, zeolites with pore diameters much smaller than the dynamic diameter of benzene, such as SAPO-34 and MOR, cannot hold benzene in their channels. The structure feature results in shape-selectivity of product, so the active site for methane aromatization can only be supplied by the external surface. Therefore, much ethylene is formed and selectivity to benzene is very low and even reaches zero. Moreover, their stability is poor and activity decreases rapidly. In case of zeolites with cages, which have three-dimensional structure, the structure is advantageous to generation of condensed ring aromatics type deposited carbon. This blocks the channel rapidly, and also causes low selectivity to aromatics and even no aromatics.

As for MCM-41, due to its large pore diameter and one-dimensional elliptical straight channel, the deposited carbon not only does not block the channel, but can modify the pore size. Thus with increasing time on stream it becomes favorable to the formation of aromatics. This speculation is confirmed by the experimental results: over the catalyst supported on MCM-41, the methane conversion and selectivity to benzene increase with increasing reaction time, and a very long induction stage exists. As far as the deactivation behavior of various catalysts is concerned, the effect of deposited carbon on the pore structure of supports is an essential factor. The different deactivation behavior over Mo/MCM-41 catalysts compared with other catalysts confirmed this. From the previous results, it can be seen that, if the channel system and pore size of zeolites are favorable to the diffusion of the reactant and product molecules, and do not have a cage structure in which the coke is readily deposited, they can maintain relatively stable activity for methane aromatization.

Based upon the above discussions, it can be concluded that H-form zeolites with two-dimensional pore structure and diameter equaling the dynamic diameter of benzene are fine supports of catalysts for methane aromatization, which is probably due to that zeolites with such structure exhibit a fine shape-selective catalytic function. Of course, as far as the methane aromatization reaction is concerned, acidity is another very important factor, so one cannot ascribe the different catalytic performance over various zeolites only to the effects of channel structure. The effect of the acidity of supports will be discussed in a separate work.

3.4. Optimization of silica–alumina zeolite catalysts

Previous studies [20] show that the optimal loading of MoO_3 over H-ZSM-5 is about 3–5%. As there is difference in crystal structure and pore system among H-ZSM-5, H-ZSM-8, H-ZSM-11 and H-β zeolite, it is necessary to investigate if the optimal loadings of MoO_3 over the last three zeolites are roughly the same as that over H-ZSM-5. The activities over MoO_3/H-ZSM-8 with different MoO_3 loadings are shown in table 4. It can be seen that the MoO_3 loading over H-ZSM-8 of about 5–6% is optimal, which is a little higher than the 3–5% optimal MoO_3 loading over H-ZSM-5. MoO_3 loading larger than 7% is not advantageous to methane aromatization and formation of C_2 over H-ZSM-8. As can be seen in table 5, the optimal MoO_3 loading over H-β-supported catalyst is about 5–7%, which is very near to that over H-ZSM-8-supported catalyst. Effect of Si/Al ratio on activity of MoO_3/H-ZSM-11 is given in table 6, from which it can be seen that with the Si/Al ratio decreasing, the activity of MoO_3/H-ZSM-11 increases. For instance, the methane conversion of MoO_3/H-ZSM-11 with $SiO_2/Al_2O_3 = 25$ is higher than that with $SiO_2/Al_2O_3 = 100$ under the same reaction conditions. That is, the higher the SiO_2/Al_2O_3 ratio, the lower the methane conversion and benzene selectivity. As is well known, the lower the SiO_2/Al_2O_3 is, the more the AlO_4 tetrahedral in zeolite framework is, and, as a result, the stronger the acidity of H-ZSM-11 is. Therefore, the change of catalyst activity with different SiO_2/Al_2O_3 ratio reflects the effect of zeolite acidity on the reaction. From table 6 it can also be found that the optimal SiO_2/Al_2O_3 ratio of H-ZSM-11 for methane aromatization is 25–50.

Table 4
Effect of MoO_3 loading on activity of MoO_3/H-ZSM-8 at 973 K.

MoO_3 loading (wt%)	Methane conversion (%)	Selectivity (%)		
		Benzene	C_2	CO
0	0.1	35.8	64.2	0
1	1.3	68.2	4.2	27.6
3	3.1	76.1	3.3	20.6
5	3.52	77.6	4.5	17.9
6	4.11	86.7	3.9	9.4
8	2.90	68.6	3.1	28.3
10	2.45	65.6	5.2	29.2

Table 5
Effect of MoO_3 loading on activity of MoO_3/H-β at 973 K.

MoO_3 loading (wt%)	Methane conversion (%)	Selectivity (%)		
		Benzene	C_2	CO
1	1.96	72.4	13.1	14.5
3	2.47	79.6	11.7	8.7
5	2.79	86.8	8.8	4.4
7	3.11	80.4	8.8	10.8
8	2.81	80.4	11.4	8.2
10	1.27	58.5	16.3	25.2

Table 6
Effect of SiO_2/Al_2O_3 ratio on activity of 3 wt% MoO_3/H-ZSM-11 at 973 K.

SiO_2/Al_2O_3 ratio	Methane conversion (%)	Selectivity (%)		
		Benzene	C_2	CO
25	8.0	90.9	5.5	3.6
50	7.61	91.6	5.3	3.1
100	6.55	90.5	5.6	3.9
200	4.48	81.9	7.6	10.5

4. Conclusions

(1) Na-form ZSM-8, ZSM-11, β and MCM-41 zeolites were synthesized by a hydrothermal crystallization method in alkaline medium, followed by ion exchange to obtain H-form zeolites. They all have nice crystallinity and are pure phase zeolites.

(2) All of these zeolites have strong IR adsorption at 1000–1100 cm^{-1} and 450 cm^{-1}. ZSM-5, ZSM-8 and ZSM-11 which consist of 5-membered rings, possess similar XRD patterns and IR spectra. The band at 550 cm^{-1} is ascribed to double 5-membered rings of ZSM-5, ZSM-8 and ZSM-11, while that band of X and Y zeolite appears in the range of 550–580 cm^{-1}.

(3) The activity order of methane aromatization over Mo-based catalysts supported on various zeolites is as follows: MoO_3/H-ZSM-11 $>$ MoO_3/H-ZSM-5 $>$ MoO_3/

H-ZSM-8 $>$ MoO_3/H-β $>$ MoO_3/H-MCM-41 $>$ MoO_3/H-SAPO-34 $\approx$ MoO_3/H-MOR $\approx$ MoO_3/H-X $\approx$ MoO_3/H-Y $>$ MoO_3/H-SAPO-5 $\approx$ MoO_3/H-SAPO-11. The maximal conversion of methane over 3% MoO_3/H-ZSM-11 at 973 K reached 8.0% with selectivity to benzene higher than 90%. Only a small amount of ethylene was observed over H-MOR-, H-X- and H-Y-supported zeolites, and no hydrocarbons were produced over H-SAPO-5- and H-SAPO-11-supported catalysts.

(4) Silica–alumina zeolites such as H-ZSM-5, H-ZSM-8, H-ZSM-11 and β zeolite, etc. with two-dimensional structure and pore size near to the dynamic diameter of benzene, $\sim$6 Å, are fine supports of Mo-based catalysts for methane aromatization. Catalysts with poor activity or no activity all do not possess or do not possess simultaneously these two features: $\sim$6 Å pore size and two-dimensional pore structure.

(5) The optimal MoO_3 loadings over H-ZSM-8 and H-β are 5–7 and 7–8%, respectively. The optimal SiO_2/Al_2O_3 ratio of H-ZSM-11 for methane aromatization reaction is 25–50.

References

[1] L. Guczi, R.A. van Santen and K.V. Sarma, Catal. Rev. Sci. Eng. 38 (1992) 249.

[2] L. Wang, L. Tai, M. Xie, G. Xu, J. Huang and Y. Xu, Catal. Lett. 21 (1993) 35.

[3] Y. Xu, S. Liu, L. Wang, M. Xie and X. Guo, Catal. Lett. 30 (1995) 135; 40 (1996) 207.

[4] L. Chen, L. Lin, Z. Xu and T. Zhang, J. Catal. 156 (1995) 190.

[5] L. Chen, L. Lin, Z. Xu and T. Zhang, J. Catal. 161 (1996) 107.

[6] D. Wang, J.H. Lunsford and M.P. Rosynek, J. Catal. 169 (1997) 347.

[7] F. Solymosi, J. Cserenyi, A. Szoke, T. Bansagi and A. Oszko, J. Catal. 165 (1997) 150.

[8] F. Solymosi, A. Erdohelyi and A. Szoke, Catal. Lett. 32 (1995) 43.

[9] J.H. Lunsford, M. Rosynek and D. Wang, Paper presented at the 14th North American Meeting of the Catalysis Society, Snowbird, 1995.

[10] F. Solymosi, A. Szoke and J. Cserenyi, Catal. Lett. 39 (1996) 157.

[11] L. Chen, L. Lin, Z. Xu, T. Zhang and X. Li, Catal. Lett. 39 (1996) 169.

[12] Y. Shu, Y. Xu, S. Wang, L. Wang and X. Guo, J. Catal. 170 (1997) 11.

[13] S. Wong, Y. Xu, L. Wang, S. Liu, G. Li, M. Xie and X. Guo, Catal. Lett. 38 (1996) 39.

[14] F. Solymosi, A. Erdohelyi and A. Szoke, Catal. Lett. 32 (1995) 43.

[15] D. Wang, J.H. Lunsford and M. Rosynek, Paper presented at the 14th Meeting of the North American Catalysis Society, Snowbird, 1995;
J.H. Lunsford, M. Rosynek and D. Wang, Paper presented at the 4th International Natural Gas Conversion, Kruger National Park, South Africa, 1995.

[16] C.J. Plank, E.J. Rosinski and M.K. Rubin, GB patent 1,334,243 (1973).

[17] G.A. Jablonski, L.B. Sand and J.A. Gard, Zeolites 6 (1986) 396.

[18] M.A. Camblor, A. Corma and J. Perez-Pariente, Zeolites 13 (1993) 82.

[19] J.S. Beck et al., J. Am. Chem. Soc. 114 (1992) 10834.

[20] L. Chen et al., J. Catal. 157 (1995) 190.